AFDEX Newsletter
Advisor for metal Forming process Design EXpert
Q4 / 2026

MFRC Metal Forming Research Corporation
www.afdex.com, mfrc@afdex.com
Tel: +82-55-755-7529, Fax: +82-55-761-7529

Contents

1. AFDEX V26R01 Release
2. AFDEX Simulation Case Studies
2.1 Asymmetric Ring Rolling Simulation
2.2 Microstructure and Hardness Prediction Improvements
2.3 Front and Rear Wheel Hub Optimization
2.4 Springback Prediction in Roll Forming
2.5 Multi-Body Tensile Test Simulation
3. Major UI Improvements
3.1 Grouped Die-Position Initialization
3.2 3D Piercing/Trimming Improvements
3.3 Postprocessor Vector Display Improvements
3.4 Automatic Die Corner Radius Correction for 2D DXF Models
3.5 Material Property Input UI Redesign
3.6 Hydraulic Press Settings in the Preprocessor
4. Notice
4.1 MFRC at ICTP 2026

1. AFDEX V26R01 Release

AFDEX V26R01 was released in late September 2026. The release includes the new features introduced in the previous quarterly newsletter, along with a range of additional capabilities presented in this issue. It also incorporates improvement requests from various customers. The AFDEX development team continues to enhance usability and simulation performance. We remain committed to delivering more accurate simulation results and a more efficient working environment.

2. AFDEX Simulation Case Studies

2.1 Asymmetric Ring Rolling Simulation

Most ring-rolled components, including bearings, have symmetric geometries. However, when a preform is produced by forging to improve productivity and cost competitiveness, an asymmetric workpiece may be unavoidable. In such cases, the material moves from side to side during ring rolling and must eventually reach an equilibrium state. Accurate finite element simulation of asymmetric ring rolling is therefore particularly important.

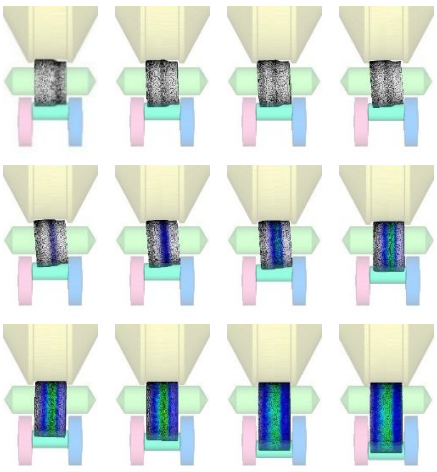


Figure 2.1. Simulation example of an asymmetric ring rolling process

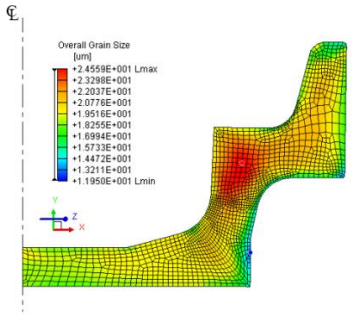
Conventional ring rolling simulation models were developed on the assumption of symmetry and are therefore unsuitable for asymmetric ring rolling. Figure 2.1 presents an asymmetric ring rolling simulation, highlighting the lateral oscillation of the workpiece.

The relative motion between the work roll and the mandrel, which drives the ring rolling process, produces a negative radial strain rate. Under the incompressibility constraint, this must be offset by the circumferential and axial strain rates, which are generally positive. These strain-rate components are not symmetric and continuously change the radial geometry of the workpiece.

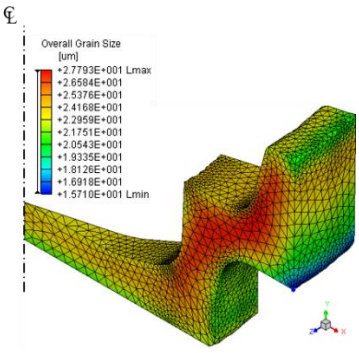
2.2 Microstructure and Hardness Prediction Improvements

Two-dimensional and three-dimensional metal forming simulation tests were conducted to validate the performance of the microstructure and hardness prediction functions.

The tests evaluated the consistency and stability of simulation results produced by the updated solver and examined potential issues and opportunities for further improvement.



(a) 2D



(b) 3D

Figure 2.2. Grain size distributions

The principal validation parameters were average grain size and material hardness. Figures 2.2(a) and 2.2(b) show the grain sizes predicted by 2D and 3D finite element analyses, respectively.

Figure 2.3 presents the hardness prediction results obtained from the 2D finite element analysis.

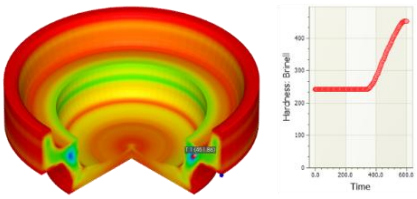


Figure 2.3 Predicted material hardness

2.3 Front and Rear Wheel Hub Optimization

A process optimization study was conducted to reduce the number of forging stages for front and rear wheel hubs from five to three. The objective was to simplify the process and improve production efficiency while maintaining the required part geometry and forming quality.

A metal forming simulation of the proposed three-stage forging process was performed to examine material deformation and formability at each stage.

Figure 2.4 shows the simulation results for the three-stage forging process, illustrating the progression of material deformation in the front and rear hubs.

Further simulations and validation will be performed to assess the feasibility of the proposed process optimization.

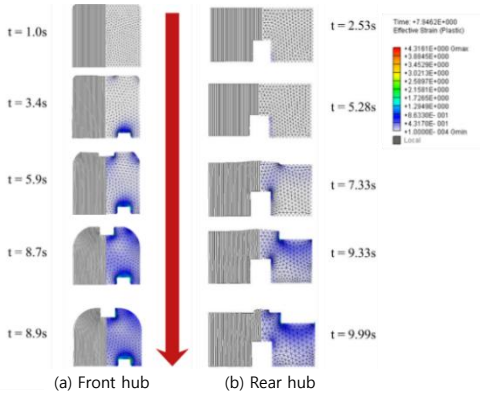


Figure 2.4 Deformation history

2.4 Springback Prediction in Roll Forming

Springback in 3D roll forming occurs when the material elastically recovers after the forming load is removed. This phenomenon significantly affects the dimensional accuracy of the final product.

The material deformation behavior during 3D roll forming and the springback characteristics after forming were analyzed to evaluate changes in product geometry and dimensions caused by elastic recovery. In particular, springback at the leading end, middle section, and trailing end of the product was compared with the target geometry to assess deviations at different locations.

Figure 2.5 shows the 3D models of the rollers and workpiece, Figure 2.6 shows the automatically generated tetrahedral mesh, and Figure 2.7 compares springback predictions at different locations along the product.

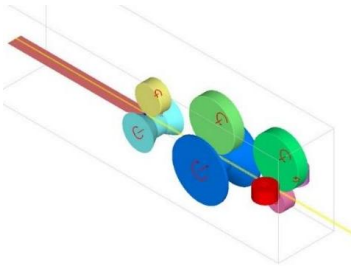


Figure 2.5. Roll forming simulation model



Figure 2.6. Automatic generation of a tetrahedral mesh

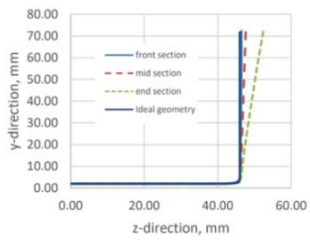


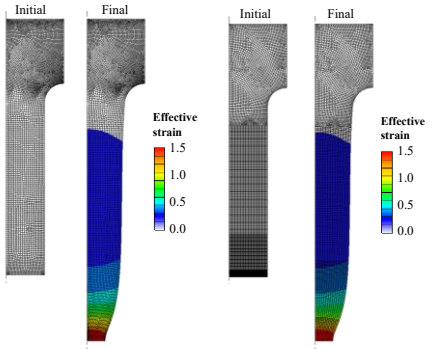
Figure 2.7. Comparison of predicted springback at different locations

2.5 Multi-Body Tensile Test Simulation

A tensile specimen can be divided into the gauge section and the regions outside the gauge section. Clearly distinguishing these regions during simulation is important, particularly when using tensile test simulations to obtain material flow properties.

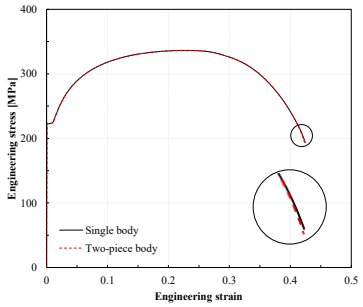
Figure 2.8 compares a single-body tensile test model with a multi-body model in which the gauge section and the other regions are treated as separate bodies. The initial simulation models, final geometries, and simulation results are compared. Both approaches produce results

that are consistent from an engineering standpoint. The multi-body approach offers significant advantages for subsequent research and applications involving a variety of tensile test conditions. AFDEX provides an efficient function for obtaining flow curves by using this capability.



Single-body Multi-body

(a) Initial simulation models and final geometries



(b) Simulation results

Figure 2.8 Comparison of single-body and multi-body tensile test models and their simulation results

3. Major UI Improvements

3.1 Grouped Die-Position Initialization

Starting with AFDEX V26R01, multi-stage simulations involving multiple dies can initialize die positions either as groups (Figure 3.1(a)) or individually (Figure 3.1(b)). This provides greater flexibility and usability when configuring die positions in complex multi-die, multi-stage processes.

In previous versions, grouped initialization was the default. When the process stage changed, die positions were initialized while preserving the relative coordinates between dies. The new individual-initialization option allows each die to be positioned independently according to the workpiece location.

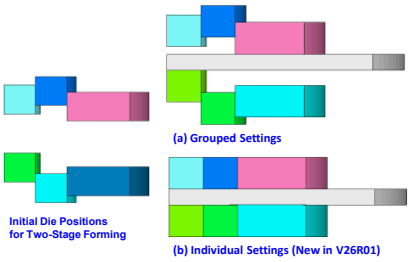


Figure 3.1 Die-position initialization

3.2 3D Piercing/Trimming Improvements

AFDEX V26R01 introduces an option to perform Boolean operations directly on the basis of die geometry during 3D piercing/trimming simulations. This simplifies simulation setup for complex piercing and trimming geometries and provides a more intuitive way to define material-removal regions.

An additional option allows users to specify independently whether the moving die and fixed die are excluded from the operation, accommodating a wider range of die configurations and process conditions (Figure 3.2). The software can also automatically extract piercing/trimming regions for use in simulation, reducing manual input and the risk of errors when selecting regions. Together, these enhancements reduce modeling and preparation time for complex 3D piercing/trimming processes while improving accuracy and workflow efficiency.

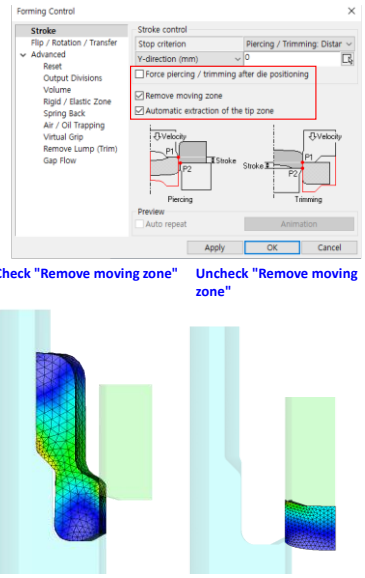


Figure 3.2 Improved piercing/trimming functions

3.3 Postprocessor Vector Display Improvements

AFDEX V26R01 adds options in the postprocessor for controlling the arrow size and display region of vector-based simulation results, including velocity fields, principal stresses, and contact pressure (Figure 3.3).

Users can adjust vector size and the displayed region to suit the mesh configuration and the characteristics of the results being visualized.

These controls help prevent visual clutter caused by overlapping or excessive vectors in complex results, making major deformation patterns and stress distributions easier to interpret. They also improve readability and visualization when examining specific regions of interest, supporting more intuitive analysis and evaluation.

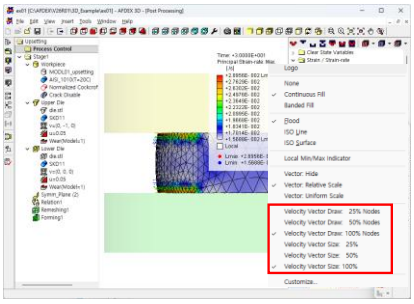


Figure 3.3. Vector display option settings

3.4 Automatic Die Corner Radius Correction for 2D DXF Models

AFDEX V26R01 introduces a feature that prompts users to apply automatic die corner-radius correction when importing a 2D CAD model (Figure 3.4). The function automatically assigns a minimum die corner radius where the CAD geometry does not provide an adequate radius, adjusting the geometry to make it suitable for simulation.

Excessively sharp die corners can lead to local mesh distortion or concentrated deformation, which may impair convergence. Automatic corner-radius correction helps mitigate these issues, improve numerical stability and convergence, and reduce unnecessary simulation interruptions and rework.

The feature also improves preparation efficiency by reducing the need to modify the CAD model manually.

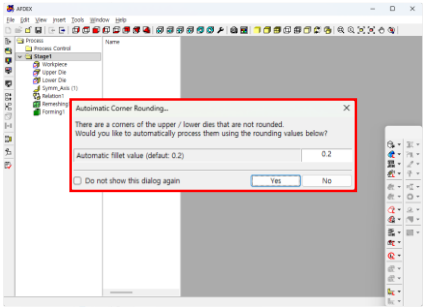


Figure 3.4. Automatic die corner radius correction

3.5 Material Property Input UI Redesign

With the addition of support for anisotropic material models in AFDEX V26R01, the material property input interface has been redesigned. The updated interface enables more systematic entry and management of material properties for both isotropic and anisotropic material models (Figure 3.5).

This improves the ease of entering data for different material models and the efficiency of material property management. Compatibility with existing material property databases is maintained, allowing users to continue using their database files without conversion or modification.

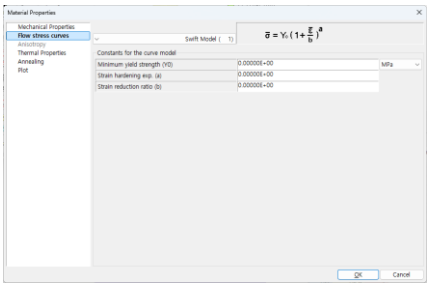


Figure 3.5. Material property input interface

3.6 Hydraulic Press Settings in the Preprocessor

AFDEX V26R01 adds a user interface for specifying hydraulic press conditions under the die velocity type settings in the preprocessor (Figure 3.6). Previously, users had to modify option values directly in the simulation input file to apply hydraulic press conditions. In the new release, these conditions can be configured more intuitively through the preprocessor interface.

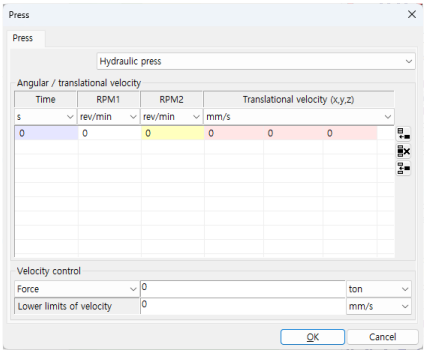


Figure 3.6 Hydraulic press condition input interface

4. Notice

4.1 MFRC at ICTP 2026

MFRC and Gyeongsang National University participated in ICTP 2026, held on October 11–16, 2026, in Jeju Island, South Korea, with Professor Jeong Hwan Yoon of KAIST serving as conference chairman. The conference brought together numerous industry experts, professors, researchers, and students from around the world to share the latest research and developments in metal forming technology.

In addition to showcasing AFDEX at the exhibition, they presented four academic papers covering (1) remeshing with consideration of simulation accuracy, (2) plate forging and anisotropy, (3) friction and abrupt changes in friction behavior, and (4) metallurgical prediction and heat treatment.

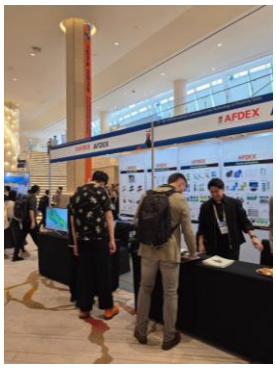


Figure 4.1 MFRC's exhibition booth at ICTP 2026